Research Article

Annals of Computational Physics and Material Science

Antimatter Enigma Solved: Astronomical Data Allows Identification of 77 Supermassive Antimatter Black Holes and 23 Antimatter Galaxies.

Policarpo Yoshin Ulianov MSc,PhD[1]*

[1]*R&D Department, PowerOpticks Tecnologia, Av. Luiz Boiteux Piazza, Florianópolis, 88056-000, SC, Brazil.*

***Corresponding Author**
Policarpo Yoshin Ulianov, R&D Department, PowerOpticks Tecnologia, Brazil.

Submitted: 2024, Jan 05; **Accepted:** 2024, Feb 20; **Published:** 2024 , Feb 29

Citation: Ulianov, P. Y. (2024). Antimatter Enigma Solved: Astronomical Data Allows Identification of 77 Supermassive Antimatter Black Holes and 23 Antimatter Galaxies. *Ann Comp Phy Material Sci, 1*(1), 01-15.

Abstract

Initial results from the Alpha-CERN antihydrogen experiment indicate no discernible difference in the gravitational behavior between matter and antimatter, challenging CP violation models. Given that antimatter exhibits the same gravitational behavior as matter, distinguishing between a supermassive black hole (SMBH) composed of matter and an antimatter supermassive black hole (ASMBH) becomes challenging, as their gravitational effects are indistinguishable. This raises the question: Could the SMBH in the Milky Way, and all observed spiral galaxies, potentially be an ASMBH, with its event horizon concealing the equivalent number of antimatter particles, thereby preventing matter-antimatter destruction within a matter galaxy?

This article assesses astronomical data comparing the mass of 100 SMBHs with their host galaxies. A theoretical value for the logarithmic mass relationship Log($M_{Stellar}$ /M_{SMBH}) is presented: 2.963 for ASMBHs situated in matter galaxies, and 2.285 for MSBHs in antimatter galaxies. This relationship, derived from the Ulianov Theory, is based on the premise of matter galaxy formation from protons and electrons expelled by ASMBHs during cosmic inflation. The same theory also posits antimatter galaxy formation from antiprotons and positrons released by matter SMBHs during this period.

The database analysis (of 100 galaxies and their respective SMBHs) revealed that 77% of the SMBHs are composed of antimatter, resulting in a logarithmic relationship value of (2.945 ± 0.018) for the Log($M_{Stellar}$/M_{ASMBH}), while 23% are composed of matter, resulting in a value of (2.267 ± 0.036) for the Log($M_{AStellar}$/M_{SMBH}). The congruence between these values and the theoretical prediction is likely not mere coincidence. A thorough examination of the results confirms the model's validity and underscores the precision of astronomers' mass measurements, with only 3 cases showing actual measurement errors beyond the predicted range. This discovery is pivotal, as it suggests the Ulianov Theory's potential to produce novel predictions, such as this model. Originating from a cold and empty universe, this model outlines the galaxy mass formation process, in which ASMBHs harness energy from cosmic inflation, converting it into matter and antimatter particles. This process is termed the "Small Bang" model by the author, reflecting its cold and gradual nature, contrasting the explosive nature of the "Big Bang".

Keywords: Antimatter, Supermassive Black Hole, Antimatter Supermassive Black Hole, Antimatter Galaxies, Antimatter Enigma, Dark Matter, Cp Violation.

1. Introduction

Antimatter is composed of antiparticles, which have properties opposite to regular matter particles. For instance, the antiproton has the opposite charge to a proton, and the positron (electron's antiparticle) carries a positive charge [1].

When matter meets its antiparticle counterpart, they annihilate each other [2]. This results in a conversion of their combined mass into energy, as described by E=mc², producing electromagnetic radiation.

The antimatter enigma stems from the prevailing theory that the Big Bang should have created equal quantities of matter and antimatter [3]. Yet, our universe exhibits a clear predominance of matter (M) over antimatter (AM). This is highlighted by the lack of large-scale particle-antiparticle annihilations, which would release vast amounts of energy and be easily observable. The widely accepted resolution to this puzzle involves M/AM asymmetry or "CP violation" [4]. "CP" stands for "charge-parity", related to charge (C) and parity (P) inversion properties. Experiments suggest potential minor variances in the behavior of particles versus antiparticles, hinting at unknown processes

during the Big Bang that might have favored matter production. However, initial findings from the Alpha-CERN antihydrogen experiment revealed no discrepancies in gravitational behavior between matter and antimatter, casting doubt on the CP violation models [5]. Furthermore, the author contends that CP violation cannot singularly account for the antimatter scarcity or elucidate matter origins and spiral galaxy formations.

Introducing an alternative to the CP violation model, the "Small Bang" theory, a component of the comprehensive Unified Theory crafted by P. Y. Ulianov over three decades, dubbed the Ulianov Theory (UT) [6-9].

A brief outline of the Small Bang model follows, with detailed descriptions available in references [10,11]:
The Small Bang theory proposes our universe started in an extremely tiny space, equivalent to the Planck length, devoid of energy (absolute zero temperature). It expanded as a 5D space-time (three spatial dimensions with two complex time dimensions) at a pace just exceeding light speed ($2\pi c$).

Eventually, this cold, expanded void witnessed the emergence of virtual particle pairs. Among these, the most energetic pairs were micro black holes (µBHs) of matter and antimatter. These µBHs briefly materialized due to quantum fluctuations before immediately annihilating each other.

During cosmic inflation, (modeled in the Small Bang theory as the "imaginary time" space "initialization") the rapid space expansion, separated some virtual Matter µBH and Antimatter µBH (MµBH / AMµBH) pairs [12]. They moved apart faster than light speed, isolating them. The AMµBH event horizons also expanded, causing antimatter µBHs to grow in mass by absorbing antimatter particles from the void space and expelling as a garage, matter particles spiral jets that will form a spiral galaxy over its central position.

In this framework, antimatter µBHs release matter streams of protons and electrons while consuming their antiparticles, positrons, and antiprotons. This allows them to expand their event horizons as they are influenced by cosmic inflation. If antimatter µBHs consumed both matter and antimatter, they wouldn't grow.

This expanding antimatter µBH eventually becomes a standard-sized antimatter BH, behaving like a spinning hose ejecting continuous streams in opposing directions, resembling a double spiral. Ultimately, it morphs into a supermassive antimatter BH, housing antiparticles equivalent to the entire spiral galaxy surrounding it.

According to the Small Bang model, this process underpins the creation of all matter galaxies. It explains the fate of antimatter (within the ASMBH) and the lack of observable energy from matter-antimatter annihilations. This is because antimatter remains ensnared within supermassive black holes in each matter galaxy, preventing any collision with typical matter.

1.1 The Formation of Galaxies in the Small Bang Theory

The Small Bang theory hypothesizes that Micro Black Holes (uBHs) originate with a mass equal to the Planck mass and a corresponding event horizon radius of the Planck length. Emerging from quantum vacuum fluctuations, these uBHs consist of virtual particle pairs, oscillating between states of matter and antimatter. These fluctuations, governed by quantum mechanics, cause these virtual particles to annihilate each other almost instantaneously, leaving a net energy of zero and causing brief fluctuations of both "positive" and "negative" energies.
In this model, space is visualized as a vacuum bubble, initially the size of a Planck length. Over billions of Planck time units, cosmic inflation, a concept rooted in the Big Bang theory, transpires. This rapid space expansion leads to numerous virtual pairs of AMuBH (Antimatter Micro Black Holes) and MuBH particles becoming separated. The rapid spatial growth prevents their annihilation, allowing them to solidify into genuine uBHs, leading to an exponential increase in their event horizon radii.

This rapid inflation causes the universe to expand at speeds far surpassing light. This expansion sees an AMuBH metamorphosing into an ASMBH (Antimatter Supermassive Black Hole), facilitating the creation of spiral galaxies comprising matter from the expanded AMuBHs.

This creation seemingly contradicts the energy conservation law by apparently generating energy and matter from nothing. Yet, cosmic inflation has a facet termed "Potential Inflation of Space-Time Energy" (PISTE). This vast energy source transforms the virtual micro Black Holes pairs into real M/AM uBHs without violating "CP" (Charge-Parity) symmetry. This conversion is credited with creating the galaxies we observe today. Over time, each uBH separates from its counterpart, evolving into a full-fledged Black Hole (BH). Tapping into PISTE energy, these BHs enlarge exponentially, evolving into Supermassive Black Holes (SMBHs), which play pivotal roles in forming surrounding spiral galaxies.

The Ulianov Theory proposes that matter repels antimatter. Even though the Alpha-CERN experiment indicates that antimatter obeys Earth's gravitational pull, the behavior near a black hole's event horizon might differ. According to this hypothesis, a rotating Antimatter Black Hole (AMBH) grows by selectively interacting with virtual Matter-Antimatter particle pairs near its event horizon. This interaction allows antimatter absorption and matter expulsion at high speeds, maintaining the system's momentum balance. Particle expulsion occurs primarily along the equatorial plane of the rotating black hole, allowing the matter to escape the black hole's gravitational clutches. In contrast, matter particles created near the poles gravitate toward the black hole, annihilating the previously absorbed antimatter, adding to the black hole's intricate dynamics. Although the Ulianov Theory suggests matter and antimatter repulsion, the Alpha CERN experiment confirms antimatter's gravitational behavior in line with Einstein's General Theory of Relativity. This behavior arises from spacetime's nature, where curved trajectories are the norm. Consequently, discerning whether a celestial entity is made of matter or antimatter purely by

observing orbits is challenging.

The Small Bang theory raises two queries regarding the role of antimatter supermassive black holes in our universe:
A. What happens to the matter micro black hole birthed alongside its antimatter counterpart?
B. Why is there a discrepancy between the mass of an ASMBH and the galaxy it engenders?
To address these questions, one must delve deeper into the Ulianov Theory and the Small Bang theory, which results in predictions that can be empirically tested:

- $Log\ (M_{Stellar}\ /\ M_{ASMBH}) = 2.963$
- $Log\ (M_{AStellar}/\ M_{SMBH}) = 2.285$

The derivation and analysis of these values will be further elaborated upon in subsequent sections of this article.

1.2 Current State of Research on SMBH

The relationship between the masses of galaxies and the supermassive black holes (SMBHs) at their cores is a dynamic field of research in astrophysics and cosmology [12-14]. A well-established empirical correlation, known as the "M-sigma relation," underpins this investigation, linking the mass of a central SMBH with the velocity dispersion of stars within the galaxy's bulge. This correlation suggests an intrinsic connection between the growth of SMBHs and the formation and evolution of their host galaxies.

Astronomers Marconi and Hunt introduced the M-sigma relation in 2003, named after the mass of the black hole (M) and the velocity dispersion (σ = sigma) of stars in the galaxy's bulge [15]. The M-sigma relation is often expressed as a power-law equation:
$\log(MBH) = \alpha + \beta * \log(\sigma)$
where:
MBH represents the mass of the SMBH.
σ is the velocity dispersion sigma of stars in the bulge.
α and β denote coefficients dependent on the galaxy sample and measurement methodology.

The numerical values within the M-sigma relation can vary based on the studied galaxy and SMBH sample [16]. However, there's a consistent trend where larger galaxies tend to possess more massive central black holes. The correlation's scatter is substantial, hinting at the potential influence of additional factors.

Key aspects regarding supermassive black holes and lingering inquiries concerning their nature and origin include [17]:
• Supermassive black holes are typically found at the centers of large galaxies.
• The time elapsed since the Big Bang is inadequate for black holes to reach billions of solar masses solely through accretion.
• Ancient quasars, exceptionally luminous celestial objects, are likely powered by supermassive black holes present since the early universe.
• Beyond their energy output, the connection between supermassive black holes and galaxy formation, as well as the broader universe's structure, is captivating.
• Intermediate-mass black holes might have emerged in the early universe from collapsing gas clouds or star collisions, potentially growing into supermassive scales through successive collisions and accretion. However, challenges arise due to the early universe's high-temperature conditions and accretion rate limitations.
• Existing explanations for supermassive black hole formation possess constraints, yielding various rival theories involving dynamic processes and primordial black holes.
• The true origin of supermassive black holes remains enigmatic, with fundamental gaps in our comprehension.
• Galaxy mass and the central supermassive black hole's mass are correlated, yet the underlying nature of this link remains partly elusive.
• Mergers among supermassive black holes are theoretically plausible but encounter obstacles due to black hole dynamics and the "final parsec problem," where orbital decay occurs too gradually for mergers to transpire within the universe's age. Certain supermassive black holes, like those in pristine spiral galaxies, defy explanations via collisions with other galaxies, hinting at alternative formation mechanisms.
• The universe's age doesn't afford black holes the time required to evolve into supermassive dimensions solely through accretion.
• Despite progress, considerable aspects concerning supermassive black holes are still unknown, with scientists anticipating unforeseen discoveries to reshape understanding.

To conclude this discussion on the significance of SMBH research, let us reflect on the perspective of eminent scientist Dr. M. Volonteri, who articulated the following assertion [12,17]:
"Supermassive black holes interest scientists for more than just their energy efficiency. Their formation and evolution are connected to the development of galaxies, and the even larger story of our entire Universe's history and structure. Solving the mystery of these cosmic giants would represent a significant step in scientists' ongoing effort to understand why things are the way they are. There are also theories about 'primordial black holes', which could have come into existence and begun growing before there were stars. But this is completely unknown territory. We don't have any observational proof to test this principle."

1.3 Calculation of SMBH-Galaxy Masses Relations

Within the framework of the Ulianov Theory (UT), both a proton and an electron are represented as one-dimensional strings, each possessing an equal length Li (determined by the length of the imaginary time axis multiplied by the speed of light). As the collapse of imaginary time unfolds (from the viewpoint of an observer experiencing real-time), these strings coil into distinct spherical membranes, harboring mass and electric charge either on their surfaces or within their volumes. Each string can be compacted (or wound) into a membrane in four distinct modes:
• 1D Mode: Strings wound around a 1D circular line with unit thickness (Planck length). This mode applies to photon membranes.
• 2D Mode: Strings wound around a 2D spherical surface with unit thickness (Planck length). This mode pertains to electron and positron membranes.
• 2.5D Mode: Strings wound around a 2D spherical surface with

thickness H PL. This mode applies to muon electron membranes.
• 3D Mode: Strings wound around a 3D spherical volume. This mode corresponds to proton and antiproton membranes, as well as tau electron membranes.
In UT, the membrane masses are conceptualized as nano black holes (nBHs), characterized by unit masses significantly smaller than the Planck mass. Consequently, the event horizon of nBH remains inaccessible (smaller than a Planck length) unless a substantial number of nBHs aggregate in a confined space, thereby forming a black hole. The number of nBHs within a given membrane is defined by Li divided by the average length of the wound membrane (typically determined by the radius of the membrane multiplied by 2π).

For instance, concerning the proton, this model allows the establishment of an inversely proportional relationship between the radius of the proton membrane (which manifests as a solid sphere) and its mass through the following expression:

$$m_{prot} = \frac{2h}{\pi\, c\, r_{prot}} \tag{1}$$

Likewise, for the muon electron case, UT models facilitate the formulation of the following relation:

$$m_{muon} = m_{elec}\, \pi \sqrt{\frac{3\pi}{4}\frac{m_{prot}}{m_{elec}}} \tag{2}$$

In the Small Bang model, the behavior of black holes (BHs) differs according to their composition, antimatter BHs (AMBHs) and matter BHs (MBHs), and how they interact with falling particles.

For AMBHs, only the 2D mode is accepted for all particles that fall within them. Consequently, when an antiproton enters an AMBH, the usual 3D packing of the antiproton is forbidden by the AMBH. As a result, the antiproton transitions from a 3D volume to a 2D surface, causing its mass to reduce to the value of a positron's mass (which equals that of an electron).

Conversely, MBHs accept only the 2.5D mode. Thus, when a proton falls into an MBH, its typical 3D packing converts to a 2.5D packing, causing a reduction in its observed mass. Similarly, when an electron falls into an MBH, its normal 2D packing transforms into a 2.5D packing, leading to an increase in its observed mass within the MBH, which becomes equivalent to the reduced proton mass. This occurs since both particles are confined to the 2.5D surface, which is the only available mode within the MBH.

In this “mass changing” model, the "mass energy" lost by the antiproton or proton upon falling into a BH is conserved by accelerating the BH's rotational speed. This, in turn, stores the "mass energy" as an increase in the BH's angular momentum energy, without resulting in a rise of the BH's mass by the total mass of the antiproton or proton that fell in it. Importantly, the angular momentum of a BH is relative to the spacetime structure itself. Consequently, the total mass energy "liberated" by antiprotons or protons within the BH, enhances the rotation of both the BH and the galaxy formed around it.

The author believes that this phenomenon, which may currently be related to a type of "dark matter" effect, contributes to galaxies rotating at higher speeds than anticipated. For instance, the ASMBH in the Milky Way's center, exhibits heightened angular momentum, generating elevated rotational speeds for the galaxy. This leads to the notion of "invisible matter" or dark matter around the Milky Way, causing it to rotate faster than predicted only by our galaxy's “luminous mass”.

The Ulianov Theory posits that all AMBHs at the centers of the matter galaxies, convert 99.9% of their original "protons mass energy" into rotational kinetic energy, accelerating their angular velocity to a value 30,30 times greater than a normal value. This acceleration, in turn, propels the galaxy itself to rotate at a higher angular velocity in the opposite direction, creating the illusion of the galaxy's mass being 5.51 times greater than actual. Similarly, the UT proposes that an MBH at the center of an antimatter galaxy, converts 99.5% of its mass-energy, into rotational kinetic energy, amplifying its angular velocity to a value 13,88 times greater. This causes the antimatter galaxy itself to rotate at an increased angular velocity in the opposite direction, fostering the impression that the galaxy's mass is 3.73 times greater than observed. Thus, differentiating an antimatter galaxy could potentially involve assessing the estimated amount of “dark matter” for each galaxy, with matter galaxies potentially displaying "dark matter" around 5.6 times the galaxy's mass, and antimatter galaxies around 3.7 times.

In the Small Bang model, the relationship between the mass of an antimatter SMBH and the mass of the matter galaxy it generates can be deduced from the particles generated at the event horizon of the rotating antimatter SMBH, during cosmic inflation. Antimatter particles are utilized by the ASMBH to exponentially increase its horizon event radius, while matter particles are expelled to form the surrounding galaxy. The equivalence of total electric charge between an ASMBH and the galaxy signifies that the same number (*N*) of proton-antiproton and electron-positron pairs are generated, during cosmic inflation.

Given N antiprotons and N positrons being "consumed" by the ASMBH, and N protons and N electrons, being expelled in opposing high-speed jets along a spiral trajectory that shapes the entire galaxy. So, the relationship between the galaxy and the ASMBH's mass can be defined as:
Mass of matter Galaxy:

$$M_{stellar} = N\,(m_p + m_e)$$

$$M_{stellar} = N\,(Rm_{pe}\,m_e + m_e)$$

$$M_{stellar} = N\,m_e\,(Rm_{pe} + 1) \quad (3)$$

Mass of ASMBH:

$$M_{ASMBH} = N\,(\,2D[m_p] + m_e)$$

$$\text{where } 2D[m_p] = m_e$$

$$M_{ASMBH} = 2\,N\,m_e \quad (4)$$

By applying Equation (4) to Equation (3):

$$M_{stellar} / M_{ASMBH} = N\,m_e\,(Rm_{pe} + 1) / (2\,N\,m_e)$$

$$M_{stellar} / M_{ASMBH} = (Rm_{pe} + 1) / 2 \quad (5)$$

$$M_{stellar} / M_{ASMBH} = 918.5$$

$$\log (M_{stellar} / M_{ASMBH}) = 2.963 \approx 3 \quad (6)$$

$$M_{stellar} \approx 1000\ M_{ASMBH}$$

Thus, the model suggests that the mass of an antimatter SMBH will be approximately 0.1% of the mass of the galaxy that it created.

For a matter SMBH, a similar process unfolds, generating N proton-antiproton and electron-positron pairs during cosmic inflation. N antiprotons and N positrons are expelled by the SMBH, contributing to the creation of an antimatter galaxy. Conversely, N protons and N electrons are "consumed" by the SMBH to expand its event horizon. As particles enter the SMBH, the proton's winding factor shifts to mode 2.5D, leading to a mass reduction of the mode 3D mass of the proton, expressed as mode 2.5D[m_p]. This reduction is calculated using the formula:

$m_p = m_e\sqrt{Rm_{pe}}$.

However, an additional factor of 3^2, related to the winding of proton strings around three types of (Ulianov Holes) uholes (similar to the normal formation of a proton through three types of quarks), results in 2.5D[m_p]: $m_p = \frac{m_e}{9}\sqrt{Rm_{pe}}$ .Additionally, the electron undergoes a transition from 2D winding to 2.5D, and its mass within the matter BH, increases and becomes equal to that of the proton (inside the MBH), i.e., 2.5D[m_e] = 2.5D[m_p]: $m_p = \frac{m_e}{9}\sqrt{Rm_{pe}}$.

In this context, the relationship between the antimatter galaxy's mass and the matter SMBH mass can be defined as follows:

Mass of antimatter Galaxy:

$$M_{stellar} = N\,(m_p + m_e)$$

$$M_{stellar} = N\,(Rm_{pe}\,m_e + m_e)$$

$$M_{stellar} = N\,m_e\,(Rm_{pe} + 1) \quad (7)$$

Mass of matter SMBH:

$$M_{SMBH} = N\,(2.5D[m_p] + 2.5D[m_e])$$

$$\text{where } 2.5D[m_e] = 2.5D[m_p] = \frac{m_e}{9}\sqrt{Rm_{pe}}\ .$$

$$M_{SMBH} = 2N\frac{m_e}{9}\sqrt{Rm_{pe}} \quad (8)$$

Applying Equation (7) to Equation (7):

$$M_{stellar} / M_{SMBH} = \frac{N\,m_e(Rm_{pe}+1)}{2N\frac{m_e}{9}\sqrt{Rm_{pe}}}$$

$$M_{stellar} / M_{SMBH} = \frac{9\,(Rm_{pe}+1)}{2\sqrt{Rm_{pe}}} \quad (9)$$

$$M_{stellar} / M_{SMBH} = 192.924$$

$$\log (M_{stellar} / M_{SMBH}) = 2.285 \quad (10)$$

Thus, according to this model, the mass of a matter SMBH will be approximately 0.5% of the mass of the antimatter galaxy that it created.

The calculations presented are founded on the Small Bang model, and the relationships derived within the Ulianov Theory's fundamental particles model, and withing Ulianov Theory's strings models and also in the true nature of time [6-8,11,18].

1.4 Validation of the UT Gravitational Model by the Next Alpha CERN Experiment

Within the Ulianov Theory (UT), space-time is conceived as a Ulianov Spheres Network (USN). One can picture the USN as a vast expanse akin to an ocean made up of crystal spheres. These spheres are under intense Planck Pressure, and they exhibit the properties of a perfect superfluid, with no viscosity.

A uniform USN has spheres (uspheres) with the same attributes: a diameter of L_p, a volume of L_p^3, and an internal pressure of P_p. This sets up a potential energy, E_p, which correlates with the Planck mass, m_p. If a usphere's internal pressure drops slightly below P_p, it collapses, making way for neighboring uspheres to expand and fill the void. On the other hand, if the pressure inside a usphere reaches N times P_p, its radius enlarges by the square root of N. This adjustment ensures equilibrium between the internal spheres pressure and surrounding pressures over the USN, maintaining a consistent pressure throughout.

From an observer's standpoint within the USN, every usphere appears uniform with a consistent diameter (LP). So, this observer perceives the USN as uniform, only noticing pressure changes when the network is distorted by matter or energy. This observer also can deduce a relative pressure and mass behavior, for the uspheres in the USN, by subtracting the values of PP and mP, obviating a zero mass and zero pressure empty space.

In the UT gravitation model, if we introduce a pair of micro black holes (one of matter and another of antimatter) in a uniform USN, they display distinct characteristics.

Drawing a simple analogy, consider a deep pool filled with water. If we place two balls in the pool (a lightweight ping pong ball representing the matter µBH and a denser iron ball symbolizing the antimatter µBH) the ping pong ball (with zero mass) would rise to the surface, while the iron ball (with two unitary mass) would sink. If we consider that the unitary water spheres mass is equal to zero the ping pong ball mass is equal to minus one (matter µBH mass = $-m_p$) and the iron ball mas is equal to one (antimatter µBH mass = $+m_p$).

So in UT model, the matter µBH has a volume of L_p^3 and a negative pressure ($-P_p$), equating to a negative mass ($-m_p$). In contrast, the antimatter µBH has a pressure of $+P_p$, resulting in a mass of m_p, but this volume remains equal to L_p^3. Note that is the point of view of an observer inside of the USN, that count distances in number of spheres to be jumped to going from one point to another.

Applying this pool analogy in the UT model but now considering the Earth's gravitational field, we can infer, that an antimatter micro black hole (AMuBH) positioned at the Earth's surface would ascend into space, like a iron ball put in the water at the pool top (low pressure, associated to the Eart surface) falls in direction to the pool bottom. However, the Alpha CERN experiment demonstrates that antihydrogen atoms fall downward and at first glance, this seems to refute the UT gravitational model [5]. Yet, a deeper analysis of the USN reveals subtleties. Given that the antimatter sphere has a specific internal pressure two times the extern2al pressure value, it can't maintain this radii state, and, its radius will grow, which in turn collapses 26 neighboring spheres (and the sphere volume goes to 27 L_p^3 and its area grow 9 times, affecting its density (that reduce to a 2/9 of it original value) and gravitational behavior, given by this equation:

$$g_{AM} = g_M \left(1 - \frac{2}{3^2}\right) \quad (11)$$

Equation (11) relates the acceleration of gravity for a matter body (g_M = 9.8 m/s^2 in the Earth's surface) and the acceleration of gravity, for an antimatter body (g_{AM} = 7.7 m/s^2 in the Earth surface) according to Ulianov Theory gravitational model.

This also means, that in UT, an antimatter µBH mass is equal to 0.77777777777777777777777777778 times the matter µBH (that in UT is equal to $-m_p$) and so one antimatter µBH has the same behavior that one matter µBH, with booths kinds of matter, "floating" from the high-pressure bottom pool (space pressure = 4.63 x 10^{113} Pa) to the "lower" pressure in the pool top (Earth surface pressure = 3.22 x 10^{104} Pa). And so the gravitational pull on antimatter as weaker than on matter, given this value g 77,77% small (7.7 m/s^2), that this author believe will be obtained in the next phases of g measure of antihydrogem atoms, in the Alpha CERN experiment. It is important to note again, that the equation (11) is a result for the antimatter bodies in a study of the antimatter micro black hole behavior for the case of empty space and the Earth's surface, where the pressures in the USN are equal to the Panck pressure or slightly below it value. In the case of a large mass of antimatter, such as an antimatter planet, the pressure in the USN will be greater than the Planck pressure (equal to PP + 1.43x10^9, for an antimatter Earth) and near of the event horizon in a supermassive antimatter black hole, the USN pressure could reach worth 2 P_p. Under these conditions, the mass of the antimatter µBH would become positive, and thus, effectively the antimatter inside of the ASMBH, would repel matter particles and attract antimatter particles, which is one of

the bases of the Small Bang model.

This can also be observed, from the point of view that the Cosmic Inflation stretches the SMBH structure (tending to increase the value of its event horizon radii), but the only way to this happens is if the ASMBH increases its antimatter mass, breaking virtual pairs particles (electrons/positrons or protons/antiprotons) and attract the antimatter particles (positron and antiprotons) that will fall into it event horizon at high speed, and so, expelling the matter particles away from the event horizon at the same speed, while maintaining constant the total system (antimatter SMBH + matter galaxy) linear and angular momentum. So, at least during the period of cosmic inflation, the antimatter SMBH needs to attract antimatter particles and repelled matter ones, but it maintains the same distortion in spacetime as one matter SMBH (but with a pressure in the USN bigger than PP).

So to confirm, the UT gravitational model, the antimatter particles' gravitational acceleration (g_{AM}) in Earth's gravitational, which will be measured in Alpha CERNE, will be near to 7.7m/s2, rather than the standard g_M value (9.8 m/s^2) observed for the matter particles.

By extending this concept, we can derive a relationship between the masses of black holes in different scales. If the relation between two micro BHs (matter and antimatter) masses has the same ratio for two supermassive BHs (matter and antimatter) masses, the following equation can be defined:

$$\log (M_{Astellar} / M_{SMBH}) / \log (M_{stellar} / M_{ASMBH}) \approx \log ((g_M - g_{AM})/g_M)$$

$$\log (M_{Astellar} / M_{SMBH}) - \log (M_{stellar} / M_{ASMBH}) \approx \log ((9.8-7.7)/9.8) \quad (12)$$

Apling equations (10) and (6) in equation (12):
2.285 – 2.963 ≈ -0.669
-0.678 ≈ -0.669
This mathematical exploration yields results that, though derived from distinct scales and methods, differ by merely 1%. That is a good clue to the true of UT model, and that it models probably will be confirmed by the next Alpha CERN results.

Even in its current nascent stage, the UT offers a tantalizing glimpse into a unified model of the universe. As it evolves, the UT model can elucidate all the enigmas of modern physics, propelling our understanding of the cosmos to unprecedented heights.

1.5 Observation of SMBH-Galaxy Masses in Astronomical Databases

In this section, the focus shifts to the observation of astronomy/ical data related to SMBHs. Numerous databases offer recorded mass values for both SMBHs and their host galaxies. If the theoretically predicted relationship between these two masses, as suggested by the Small Bang model and presented in equation (6), were a fixed factor of 1000, astronomers would likely have noticed this correlation long ago. However, without such a direct relationship, astronomers have established alternative connections, such as the M-sigma factor discussed in Section 3.

In the context of this topic, an examination of articles reveals tables containing observed and calculated mass values for SMBHs and their associated galaxies [19]. In the provided article, authored by H. Suh et al., the selection of their sample of 100 MBHs is described as follows:
"We investigate the cosmic evolution of the ratio between black hole (BH) mass (MBH) and host galaxy total stellar mass (Mstellar) out to z ∼ 2.5 for a sample of 100 X-ray-selected moderate-luminosity, broad-line active galactic nuclei (AGNs) in the Chandra-COSMOS Legacy Survey... We obtain 100 broad-line AGNs covering the redshift range z = 0–2.5."

The table from Dr. Suh's research consists of 100 rows, each containing the following information:
• Column A: Object ID - Identification of the object.
• Column B: Redshift - Redshift of the spectral lines.
• Column C: log MBH - Logarithm of the SMBH mass in terms of solar mass (MΘ) derived using the virial method. Values are provided with two decimal places and a single associated error range (±error).
• Column D: log Lbol - Logarithm of AGN bolometric luminosity.
• Column E: log Mstellar - Logarithm of the total stellar mass in terms of solar mass (MΘ) derived from SED fitting. Values are provided with two decimal places and an error range [-error, +error].
• Column F: Instrument - Instrument used for spectroscopy.
• Column H: Line - Broad emission line utilized.

The author then obtained these astronomical data table from, appending an additional initial column with line numbers to assign a unique point number to each SMBH and its corresponding galaxy [19]. The complete dataset, the calculations and analysis, made by the author, and all graphics presented here, can be accessed in a excel table available at [20].

Table 1 illustrates an example of the utilized data, with three points highlighted in red to indicate potential issues in the reported errors theorical mass errors.

Line Num.	Object ID	Redshift	log Lbol	log MBH		log Mstellar			Instrument	Line
				Value	± error	Value	- error	+error		
1	cid_36	1.826	45.63	9.38	0.06	12.18	0.04	0	DEIMOS	Mg II
2	cid_61	1.478	45.38	8.62	0	11.48	0.15	0	DEIMOS	Mg II
3	cid_66	1.512	45.77	8.45	0.03	11.21	0.01	0.24	DEIMOS	Mg II
12	cid_142	0.699	45.5	8.43	0.16	11.25	2.84	0	DEIMOS	Hβ
21	cid_358	0.372	45.61	8.32	0.11	10.66	1.17	0	DEIMOS	Hα
24	cid_175	1.627	45.51	8.47	0.77	11.09	0.03	0.18	DEIMOS	Mg II
30	cid_481	2.283	45.68	8.72	0.01	11.22	0.06	0.12	DEIMOS	Mg II
34	cid_512	1.516	45.98	8.41	0.06	11.99	0.09	0.06	FMOS	Hα
41	cid_566	1.458	45.84	8.87	0.1	10.99	0.38	0.06	DEIMOS	Mg II
62	cid_1174	0.088	45.58	5.85	0.01	8.01	0	0	DEIMOS	Hα
69	cid_2564	2.01	45.29	8.47	0.07	11.02	0.02	0.03	DEIMOS	Mg II
76	lid_338	1.209	45.83	8.06	0.01	11.57	0.23	0	DEIMOS	Mg II
95	lid_1538	1.523	46.03	8.19	0.05	11.84	0.06	0.06	FMOS	Hα
99	lid_1878	1.608	45.69	8.9	0.02	11.67	0.04	0	FMOS	Hα
100	lid_3456	2.146	45.03	8.02	0.57	11.87	0.06	0	DEIMOS	Mg II

Table 1: selection of lines illustrating the complete used data table presented [19]. Three points highlighted in red point out instances where reported errors in the table might have posed issues.

Figure 1(a) presents a plot with points defined by the logarithm of the galaxy's mass (log Mstellar) against the logarithm of the MBH's mass (log MBH). The orange dashed line represents the theoretically expected relationship (log MBH = log Mstellar - 2.963), while the blue line signifies the relationship derived from linear interpolation of the 100 points. The interpolation yields the equation ($Log(M_{SMBH})= 0.672\ Log\ (M_{Stellar})+ 0.9142$), which significantly diverges from the expected theoretical value.

Figure 1(b) depicts a plot featuring 100 values for the ratio ($log(M_{Stellar}\ /M_{SMBH}$). In theory, this plot should manifest as a straight line of points situated at the y-coordinate of 3.0. However, instead of this anticipated linearity, scattered points are observed within a range spanning from 1.5 to 3.8. This observation indicates a variable ($M_{Stellar}/M_{SMBH}$) ratio spanning, from 32 to 6300, an approximately 200-fold variation. This is in contrast to the predicted fixed ratio of 2.964 given by equation (6).

Upon examining the graphs in Figure 1, it becomes apparent that the theoretical relationships proposed by the Ulianov Theory,

and Small Bang models, between galaxy mass and SMBH mass are not reflected in actual astronomical data.

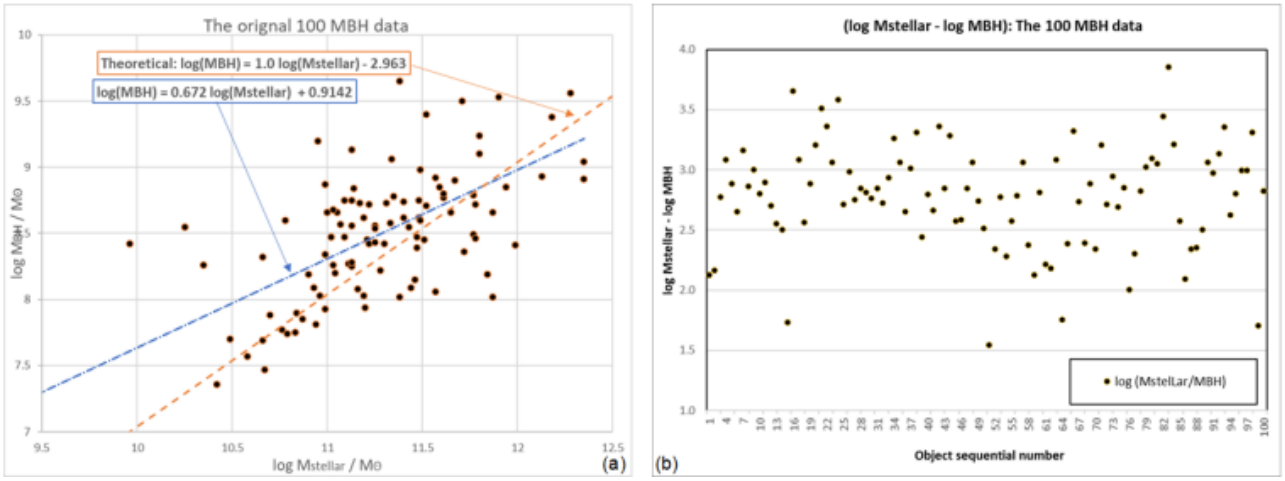

Figure 1: a) Graph illustrating a logarithmic plane, depicting the mass of each SMBH in relation to the mass of its respective galaxy; b) Logarithm of the ratio (Mstellar / MBH).

However, before dismissing the Small Bang model, it's crucial to acknowledge the existence of both highly accurate and less accurate mass values within the dataset of 100 points representing SMBH mass and galaxy mass. Some of these values exhibit remarkably low mass total errors, measuring less than 0.1. Conversely, there are instances of larger error values, such as those highlighted in Table 1 for points 24, 21, and 12. These points have corresponding maximum errors of 0.77, 1.17, and a substantial 2.84, rendering them significantly erroneous and practically invalidating their inclusion in the graphs and calculations. To account for these theoretical mass measurement errors introduced by optical instruments (referred to as mass errors), an analysis of the logarithm-subtracted graph was conducted. The goal was to estimate a theoretical maximum mass measurement error for each data point. This generates a log(mass) total error, associated with the log(mass) subtraction:

$$Log(M_{Stellar}/M_{SMBH}) = Log(M_{Stellar}) - \mathrm{Log}(M_{SMBH}) \qquad (13)$$

The calculation of the mass total error was a straightforward process, involving the addition of errors attributed to $Log(M_{SMBH})$ mass (±error, from Table 1) and the average error associated with $Log(M_{Stellar})$ mass (+error and -error, from Table 1), for all 100 points in the dataset. Once this estimated mass total error was determined, the complete set of data points was reorganized in ascending order based on this total error. This reorganization led to a new visual representation of the points on the graph in Figure 1(b), which is presented in this revised arrangement in Figure 2(a).

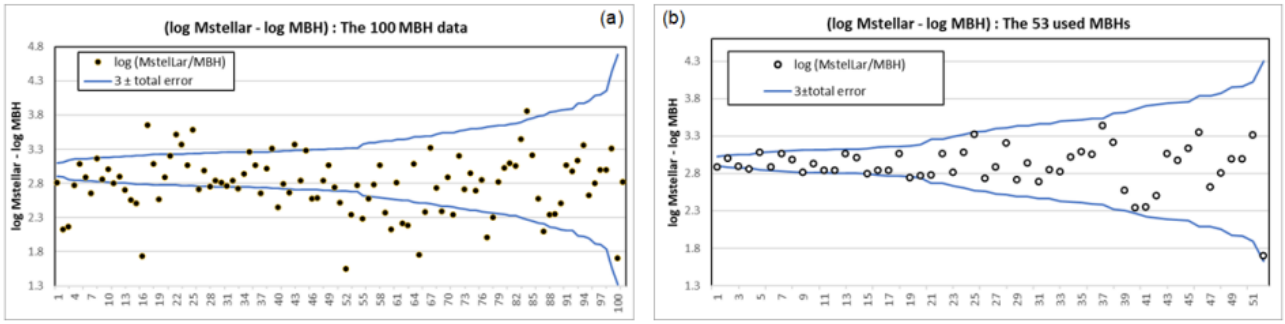

Figure 2: a) Graph depicting the logarithm of the ratio (Mstellar / MBH) with points ordered based on the maximum total error in each measurement. b) Same graph with only 53 points selected within the range of 3 ± total error.

Upon conducting this analysis of the reorganized data, two distinct groups of points become apparent: the first group includes 54 points (used MBH points) falling within the range defined by the blue lines (3+total error and 3-total error) as depicted in Figure 2(b), while the second group consists of 47 points (unused MBH pointes), lying outside this range, as illustrated in Figure 3(a).

Within the blue range, the used points, consistently converge towards a value near 3.00, with random errors falling within the ± total error range. This suggests that ideally, all 54 used points within this range should converge to the theoretical value

of 2.963, deviating from it due to random measurement errors. As the actual relation between galaxy mass and ASMBH mass can be expressed as $Log(M_{Stellar[pt]} / M_{ASMBH[pt]}) = 2.963$, a new concept of measurement error can be introduced to this dataset. For each Antimatter SMBH point (pt), this measurement error can be calculated using the formula:

$$Measur_{error[pt]} = 2.964 - \left(Log\left(M_{Stellar}[pt]\right) - Log\left(M_{ASMBH}[pt]\right)\right) \quad (14)$$

Upon closer examination of these newly calculated measurement errors and the total errors associated with the 47 unused points (as shown in Figure 3(b)), it becomes evident that several points exhibit relatively high measurement errors. However, a significant proportion of these 47 points fall within a measurement error limit below (total error + 0.2).

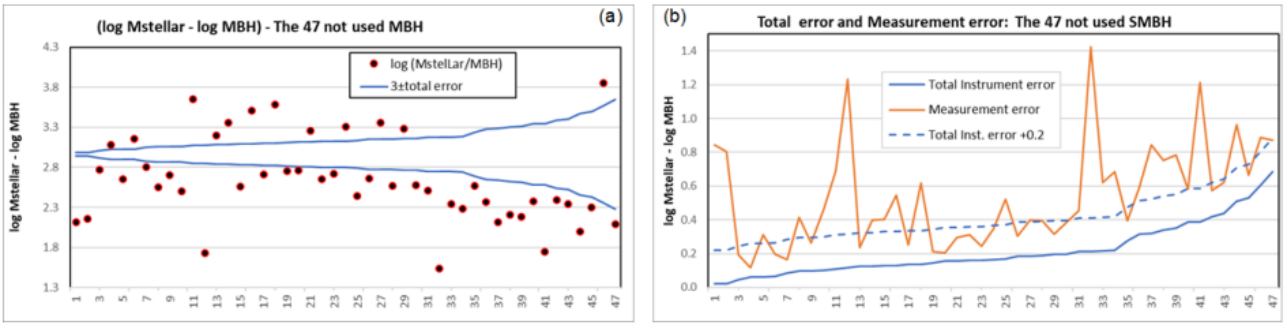

Figure 3: a) Same graph as in 2(b) with the remaining 47 points selected outside the range of 3 ± total error; b) Graph depicting the total error and theoretical measurement error for the 47 points from Figure 3(a).

This new analysis, has successfully identified 77 points that fall within the range of 2.963 ± (total error + 0.2), allowing us to classify them as antimatter SMBHs. This classification aligns with the theoretical relation of 2.963, which was calculated in section 4 based on the UT model of ASMBHs behavior.

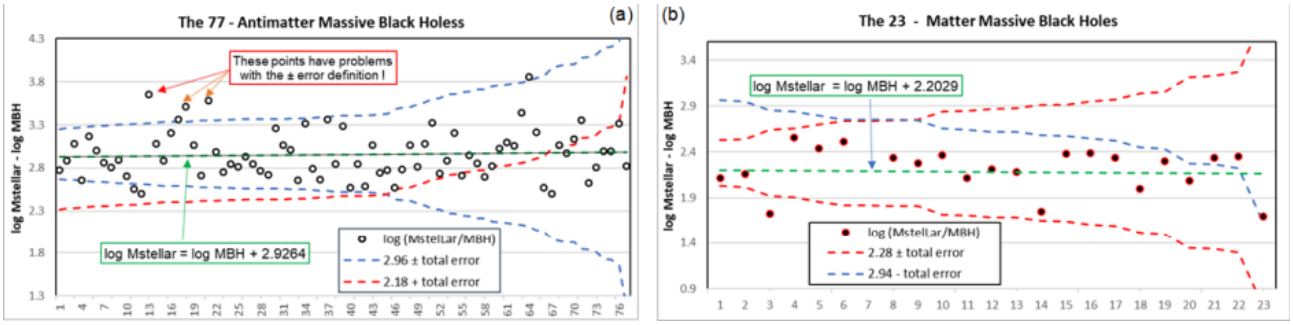

Figure 4: a) Graph showing the logarithm of the (Mstellar / MBH) ratio with points arranged based on the total theorical error in each mass measurement, featuring 77 points classified as antimatter SMBHs. b) Same graph as in 4(a) with the remaining 23 points defined as matter SMBHs selected within a range of 2.28 ± total error.

This classification can accurately be applied to 74 of the used points. However, it's worth noting that 3 used points (points 34, 76, and 95 in Table 1, indicated in red to highlight their total errors) displayed mass total errors initially reported as 0.20. Upon recalculating the measurement errors, we found them to be 0.60, three times greater than the theoretical mass total error initially calculated by the astronomers who compiled the 100 MBH data set.

For the remaining 23 unused points, they will be considered as matter SMBHs. As such, a new measurement error for these matter galaxies can be calculated using the formula:

$$Measur_{error[pt]} = 2.285 - \left(Log\left(M_{AStellar}[pt]\right) - Log\left(M_{SMBH}[pt]\right)\right) \quad (15)$$

Figures 5(a) and 5(b) depict the new measurement errors alongside the standard mass total errors for all 100 points. These graphics show that a total of 75 points possess measurement errors smaller than the predicted mass total errors. Among them, 22 points fall within the range of [total error to total error + 0.2]. Only three points, as previously mentioned, exhibited discrepancies between the standard mass total error and the new measured mass error.

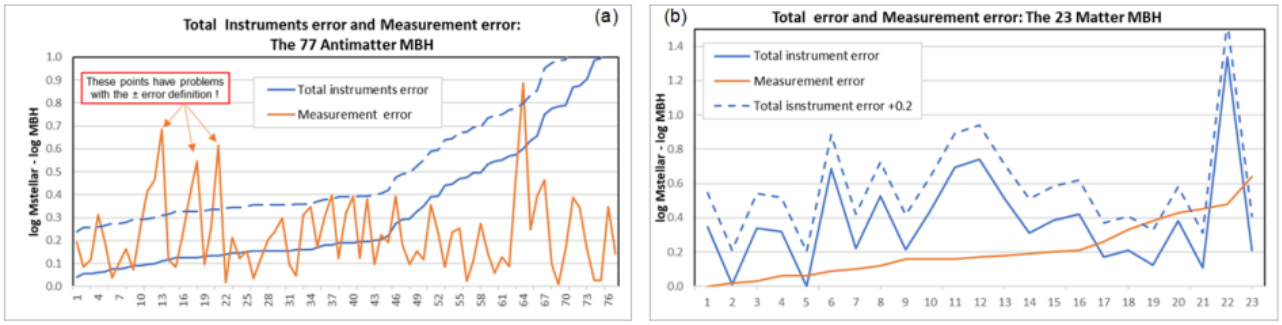

Figure 5: a) Graph showing the total error and the theoretically defined measurement error for the 77 antimatter SMBHs. b) Same graph as in 5(a), but for the 23 matter SMBHs.

With this additional error correction, 24 more points can be classified as antimatter SMBHs, generating a total of 77 identified ASMBH, as shown in Figure 5(a), while the remaining 23 points are classified as matter SMBHs placed in antimatter galaxies, as presented in Figure 5(b). Thus, the data table was divided into two groups: a matter galaxies table (MGT) with 77 points and an antimatter galaxies table (AMGT) with 23 points.

After excluding 33% of the points with higher mass errors (greater than 0.26) from each table, a total of 66 mass points (50 points in MGT and 16 points in AMGT) were utilized to create the graphs in Figure 6. These graphs reveal that, by separating the SMBHs into two distinct groups and removing the points with higher mass total errors, a nearly perfect correlation between the theoretical orange lines and the interpolated blue lines becomes apparent, as depicted in Figures 6(a) and 6(b).

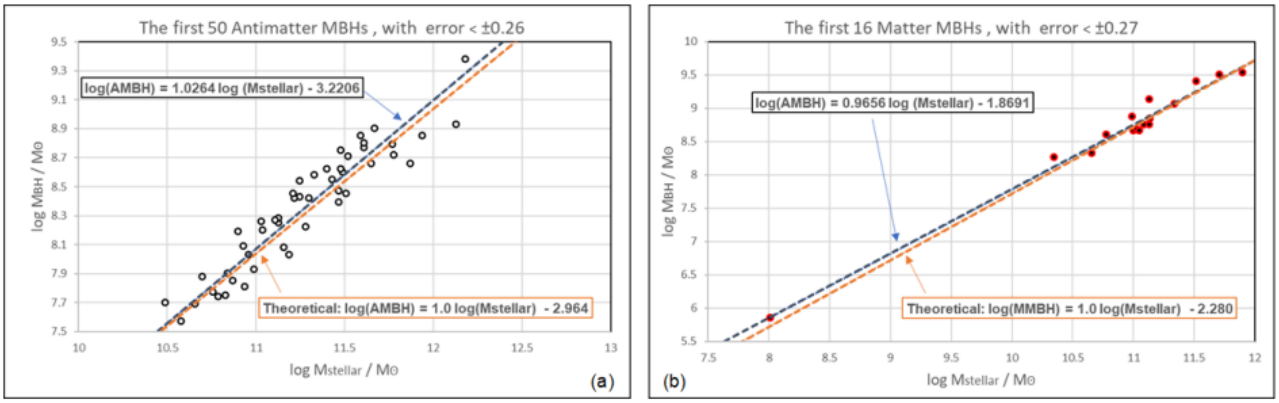

Figure 6: a) Graph showing a logarithmic plot with the mass of 50 antimatter SMBHs relative to the mass of their host galaxies. Only 50 points from the Antimatter SMBH - Matter Galaxy Table (out of 77 available) were used where the total error is less than ±0.26; b) Graph showing a logarithmic plot with the mass of 16 matter SMBHs relative to the mass of their host galaxies of antimatter. Only 16 points from the Matter SMBH - Antimatter Galaxy Table (out of 23 available) were used, where the total error is less than ±0.27.

Finally, Figure 7 visually represents the division between matter and antimatter SMBHs in relation to their relationships with galaxy masses using all 100 data points. The distinction between the theoretical lines (in orange) and the interpolated lines (in blue) is more pronounced here, as the inclusion of high error points contributes to errors in the blue interpolated lines. Moreover, it's clear from the plot that two distinct groupings exist, confirming the division between matter and antimatter galaxies. This observation is further supported by this dataset of 100 points.

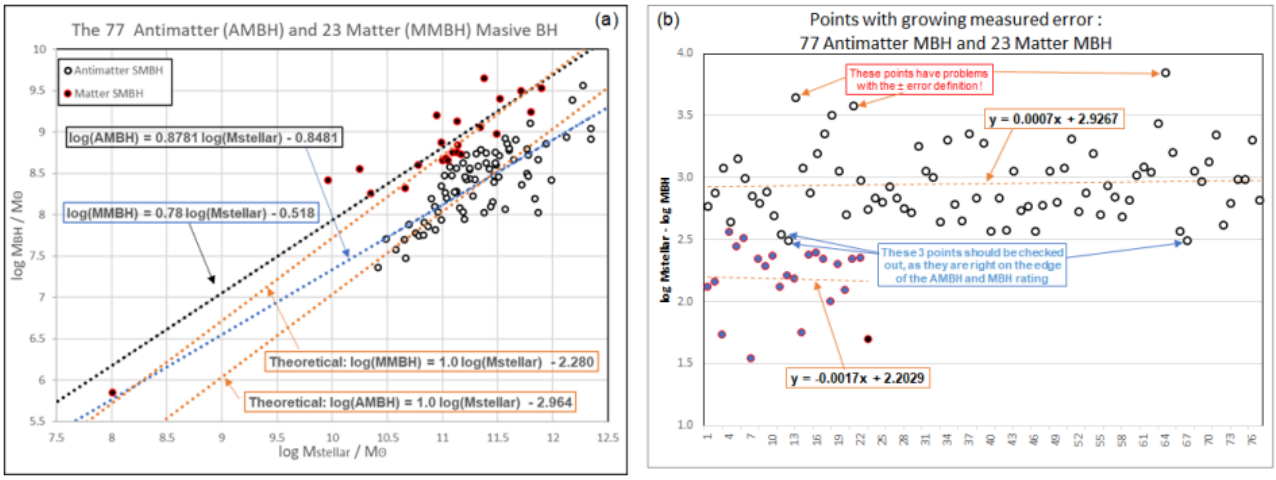

Figure 7: a) Graph showing a logarithmic plot with the mass of each type of SMBH relative to the mass of its host galaxy; b) Logarithm of the ratio (Mstellar / MBH) for the two types of SMBHs.

In Figure 7(a), it becomes apparent that antimatter galaxies are not only smaller but also less abundant compared to matter galaxies. This observation aligns with the Small Bang hypothesis, suggesting that the growth of matter µBHs is slower, leading to the formation of smaller antimatter galaxies, and that matter µBH have a higher probability of annihilation due to collisions with larger-mass antimatter µBHs. This characteristic is evident in Figure 8, where galaxies are arranged according to their names, masses and redshifts. Antimatter galaxies are positioned at the lower end, and as the mass increases, about 90% of the galaxies transition to being matter galaxies, in accordance with the predictions of the Small Bang model.

Regarding the mass of matter SMBHs, which are responsible for generating antimatter galaxies, their mass distribution should resemble that of the antimatter galaxies they inhabit. However, despite the slower growth rate of µBHs, the observed mass within them (for the same number of absorbed particles) is five times greater. Consequently, matter SMBHs occupy an intermediate position in the mass ranking, as depicted in Figure 8.

The classification of objects based on names and redshifts provides insight into the proximity of galaxies in angular direction (as similar names usually indicate nearby regions) and distance (matching redshifts). From Figure 8, it can be inferred that antimatter galaxies [cid_399, cid_340, cid_346] are likely part of the same cluster. Given that the analysis involves a sample of only 100 observed galaxies, distributed across a vast spatial volume, it explains the observation of a single cluster of antimatter galaxies. Thus, the present analysis warrants extension to the entire available database, comprising thousands of galaxies, to confirm whether these galaxies are indeed distributed in isolated clusters of the same type, as predicted by the Small Bang model.

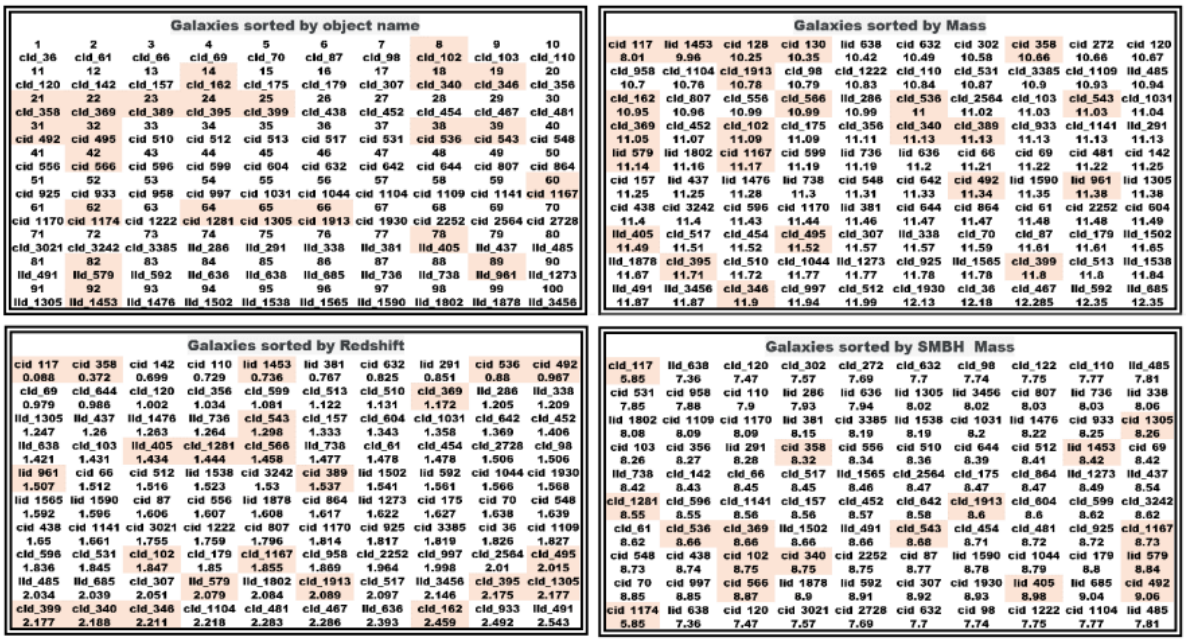

Galaxies sorted by object name

1	2	3	4	5	6	7	8	9	10
cid_36	cid_61	cid_66	cid_69	cid_70	cid_87	cid_98	cid_102	cid_103	cid_110
11	12	13	14	15	16	17	18	19	20
cid_120	cid_142	cid_157	cid_162	cid_175	cid_179	cid_307	cid_340	cid_346	cid_356
21	22	23	24	25	26	27	28	29	30
cid_358	cid_369	cid_389	cid_395	cid_399	cid_438	cid_452	cid_454	cid_467	cid_481
31	32	33	34	35	36	37	38	39	40
cid_492	cid_495	cid_510	cid_512	cid_513	cid_517	cid_531	cid_536	cid_543	cid_548
41	42	43	44	45	46	47	48	49	50
cid_556	cid_566	cid_596	cid_599	cid_604	cid_632	cid_642	cid_644	cid_807	cid_864
51	52	53	54	55	56	57	58	59	60
cid_925	cid_933	cid_958	cid_997	cid_1031	cid_1044	cid_1104	cid_1109	cid_1141	cid_1167
61	62	63	64	65	66	67	68	69	70
cid_1170	cid_1174	cid_1222	cid_1281	cid_1305	cid_1913	cid_1930	cid_2252	cid_2564	cid_2728
71	72	73	74	75	76	77	78	79	80
cid_3021	cid_3242	cid_3385	lid_286	lid_291	lid_338	lid_381	lid_405	lid_437	lid_485
81	82	83	84	85	86	87	88	89	90
lid_491	lid_579	lid_592	lid_636	lid_638	lid_685	lid_736	lid_738	lid_961	lid_1273
91	92	93	94	95	96	97	98	99	100
lid_1305	lid_1453	lid_1476	lid_1502	lid_1538	lid_1565	lid_1590	lid_1802	lid_1878	lid_3456

Galaxies sorted by Mass

cid_117	lid_1453	cid_128	cid_130	lid_638	cid_632	cid_302	cid_358	cid_272	cid_120
8.01	9.96	10.25	10.35	10.42	10.49	10.58	10.66	10.66	10.67
cid_958	cid_1104	cid_1913	cid_98	cid_1222	cid_110	cid_531	cid_3385	cid_1109	lid_485
10.7	10.76	10.78	10.79	10.83	10.84	10.87	10.9	10.93	10.94
cid_162	cid_807	cid_556	cid_566	lid_286	cid_536	cid_2564	cid_103	cid_543	cid_1031
10.95	10.96	10.99	10.99	10.99	11	11.02	11.03	11.03	11.04
cid_369	cid_452	cid_102	cid_175	cid_356	cid_340	cid_389	cid_933	cid_1141	lid_291
11.05	11.07	11.09	11.09	11.11	11.13	11.13	11.13	11.13	11.13
lid_579	lid_1802	cid_1167	cid_599	lid_736	lid_636	cid_66	cid_69	cid_481	cid_142
11.14	11.16	11.17	11.19	11.19	11.2	11.21	11.22	11.22	11.25
cid_157	lid_437	lid_1476	lid_738	cid_548	cid_642	cid_492	lid_1590	lid_961	lid_1305
11.25	11.25	11.28	11.3	11.31	11.33	11.34	11.35	11.38	11.38
cid_438	cid_3242	cid_596	cid_1170	lid_381	cid_644	cid_864	cid_61	cid_2252	cid_604
11.4	11.4	11.43	11.44	11.46	11.47	11.47	11.48	11.48	11.49
lid_405	cid_517	cid_454	cid_495	cid_307	lid_338	cid_70	cid_87	cid_179	lid_1502
11.49	11.51	11.52	11.52	11.57	11.57	11.59	11.61	11.61	11.65
lid_1878	cid_395	cid_510	cid_1044	lid_1273	cid_925	lid_1565	cid_399	cid_513	lid_1538
11.67	11.71	11.72	11.77	11.77	11.78	11.78	11.8	11.8	11.84
lid_491	lid_3456	cid_346	cid_997	cid_512	cid_1930	cid_36	cid_467	lid_592	lid_685
11.87	11.87	11.9	11.94	11.99	12.13	12.18	12.285	12.35	12.35

Galaxies sorted by Redshift

cid_117	cid_358	cid_142	cid_110	lid_1453	lid_381	cid_632	lid_291	cid_536	cid_492
0.088	0.372	0.699	0.729	0.736	0.767	0.825	0.851	0.88	0.967
cid_69	cid_644	cid_120	cid_356	cid_599	cid_513	cid_510	cid_369	lid_286	lid_338
0.979	0.986	1.002	1.034	1.081	1.122	1.131	1.172	1.205	1.209
lid_1305	lid_437	lid_1476	lid_736	cid_543	cid_157	cid_604	cid_1031	cid_642	cid_452
1.247	1.26	1.263	1.264	1.298	1.333	1.343	1.358	1.369	1.406
lid_638	cid_103	lid_405	cid_1281	cid_566	lid_738	cid_61	cid_454	cid_2728	cid_98
1.421	1.431	1.434	1.444	1.458	1.477	1.478	1.478	1.506	1.506
lid_961	cid_66	cid_512	lid_1538	cid_3242	cid_389	lid_1502	lid_592	cid_1044	cid_1930
1.507	1.512	1.516	1.523	1.53	1.537	1.541	1.561	1.566	1.568
lid_1565	lid_1590	cid_87	cid_556	lid_1878	cid_864	lid_1273	cid_175	cid_70	cid_548
1.592	1.596	1.606	1.607	1.608	1.617	1.622	1.627	1.638	1.639
cid_438	cid_1141	cid_3021	cid_1222	cid_807	cid_1170	cid_925	cid_3385	cid_36	cid_1109
1.65	1.661	1.755	1.759	1.796	1.814	1.817	1.819	1.826	1.827
cid_596	cid_531	cid_102	cid_179	cid_1167	cid_958	cid_2252	cid_997	cid_2564	cid_495
1.836	1.845	1.847	1.85	1.855	1.869	1.964	1.998	2.01	2.015
lid_485	lid_685	cid_307	lid_579	lid_1802	cid_1913	cid_517	lid_3456	cid_395	cid_1305
2.034	2.039	2.051	2.079	2.084	2.089	2.097	2.146	2.175	2.177
cid_399	cid_340	cid_346	cid_1104	cid_481	cid_467	lid_636	cid_162	cid_933	lid_491
2.177	2.188	2.211	2.218	2.283	2.286	2.393	2.459	2.492	2.543

Galaxies sorted by SMBH Mass

cid_117	lid_638	cid_120	cid_302	cid_272	cid_632	cid_98	cid_122	cid_110	lid_485
5.85	7.36	7.47	7.57	7.69	7.7	7.74	7.75	7.77	7.81
cid_531	cid_958	cid_110	lid_286	lid_636	lid_1305	lid_3456	cid_807	lid_736	lid_338
7.85	7.88	7.9	7.93	7.94	8.02	8.02	8.03	8.03	8.06
lid_1802	cid_1109	cid_1170	lid_381	cid_3385	lid_1538	cid_1031	lid_1476	cid_933	cid_1305
8.08	8.09	8.09	8.15	8.19	8.19	8.2	8.22	8.25	8.26
cid_103	cid_356	lid_291	cid_358	cid_556	cid_510	cid_644	cid_512	lid_1453	cid_69
8.26	8.27	8.28	8.32	8.34	8.36	8.39	8.41	8.42	8.42
lid_738	cid_142	cid_66	cid_517	lid_1565	cid_2564	cid_175	cid_864	lid_1273	lid_437
8.42	8.43	8.45	8.45	8.46	8.47	8.47	8.47	8.49	8.54
cid_1281	cid_596	cid_1141	cid_157	cid_452	cid_642	cid_1913	cid_604	cid_599	cid_3242
8.55	8.55	8.56	8.56	8.57	8.58	8.6	8.6	8.62	8.62
cid_61	cid_536	cid_369	lid_1502	lid_491	cid_543	cid_454	cid_481	cid_925	cid_1167
8.62	8.66	8.66	8.66	8.66	8.68	8.71	8.72	8.72	8.73
cid_548	cid_438	cid_102	cid_340	cid_2252	cid_87	lid_1590	cid_1044	cid_179	lid_579
8.73	8.74	8.75	8.75	8.75	8.77	8.78	8.79	8.8	8.84
cid_70	cid_997	cid_566	lid_1878	lid_592	cid_307	cid_1930	lid_405	lid_685	cid_492
8.85	8.85	8.87	8.9	8.91	8.92	8.93	8.98	9.04	9.06
cid_1174	lid_638	cid_120	cid_3021	cid_2728	cid_632	cid_98	cid_1222	cid_1104	lid_485
5.85	7.36	7.47	7.57	7.69	7.7	7.74	7.75	7.77	7.81

Figure 8: The 100 galaxies sorted by name, galaxy mass, SMBH mss, and redshift. Galaxies of antimatter have a colored background for the text, while galaxies of matter have a white background for the text.

In these dataset analysis conclusions, these observations lead us to acknowledge that the theoretical relationships proposed by the Ulianov Theory and Small Bang models, for galaxy and SMBH mass are indeed observed in real astronomical data.

From the values of the $Log(M_{Stellar}/M_{ASMBH})$, for the 77 matter galaxies and the vales of $Log(M_{AStellar}/M_{SMBH})$, for the 23 antimatter galaxies, we applied a weighting filter, based on the kneed theoretical total error.

The weighting factor for each galaxy can be calculated using:

$$weight_i = \frac{1}{totalerror_i^2} \tag{15}$$

The weighted mean of the logarithm ratio $Log_{W_{mean}}(M_{Stellar}/M_{ASMBH})$, is given by:

$$Log_{Wmean}(M_{Steller}/M_{SMBH}) = \frac{\sum_i \frac{1}{total\_error i^2} X \log((M_{Steller[i]}/M_{SMBH[i]})}{\sum_i \frac{1}{total\_error i^2}} \tag{16}$$

Using equation (16), for the 77 matter galaxies we find:

$$Log_{Wmean}(\frac{M_{Stellar}}{M_{ASMBH}}) = 2.945 \pm 0.018,$$

yielding a range of [2.927 to 2.963] which encompasses the 2.963 theoretical value.

Using equation (16), for the 23 antimatter galaxies we find:

$$Log_{Wmean}(\frac{M_{AStellar}}{M_{SMBH}}) = 2.267 \pm 0.036,$$

yielding a range of [2.231 to 2.302] which encompasses the 2.285 theoretical value.

So, the data analysis lends support to the Small Bang model's predictions about, the growth of matter and antimatter SMBHs, with distinct characteristics exhibited by both types. However, to validate these findings and assess whether galaxies do indeed cluster into isolated groups of matter and antimatter galaxies, a more extensive analysis involving a larger dataset is necessary.

2. Conclusion

In this article, we explore the correlation between galaxy masses and antimatter supermassive black hole (ASMBH) masses, emphasizing the implications drawn from the Ulianov Theory (UT) equations. Our close analysis of Figures 5(a) and 5(b) revealed that measurement errors, based on UT equations (14) and (15), typically matched or exceeded the anticipated total mass errors derived from optical instruments across the 97 data points studied (with three points being expended, due to their theoretical error values being outside of the observed error range).

The analysis presented in this article, brings us to two primary observations:

• **Precision in Optical Measurements:** The measured errors experts behind the theoretical erros providing together with the dataset. For a significant 97% of the data points, the computed random measurement error, rooted in the Small Bang model, aligns seamlessly with the predicted error range from optical instruments. Only in 3% of the cases was there a notable divergence from the expected values. Such a high degree of accuracy in 97% of the error estimates, given the intricacies of optical measurements, is laudable. This precision is further evident in Figure 5, which spotlights only three marked deviations.

• **Reaffirmation of the Small Bang Model:** The demonstrated accuracy in optical instrument measurements boosts our confidence in the predictions of the Small Bang model. Specific values of log(Mstellar/MAMBH) hold true for the majority of the analyzed SMBH cases, except for a few anomalies like the cid_512, lid_338, and lid_1538 objects. Furthermore, certain galaxies, such as cid_2564, cid_556, and cid_481, appear to sit on the borderline between matter and antimatter classifications, suggesting further scrutiny is required.

Moreover, we ascertained that while matter and antimatter µBHs exhibit similar mass growth trajectories, matter-dominated galaxies inherently possess substantially more mass. This phenomenon results in the obliteration of matter µBHs upon their collision with antimatter µBHs, elucidating the observed discrepancy in the ratios: 3.3 times more matter galaxies as compared to antimatter galaxies.

Even though existing astronomical data remains inconclusive about collisions between these two galaxy types, the Small Bang theory postulates distinct clustering behaviors for each. Using the methodology delineated in this work, astronomers can classify spiral galaxies and verify these assertions. The Small Bang model also implies that stars within a galaxy are homogenous in terms of mass type, a detail currently elusive to astronomical methodologies.

Figure 7(a) underscores the potential existence of two distinct

SMBH categories, each influencing the kind of galaxies they cultivate. Points in this figure cluster around two separate interpolation lines, suggesting the existence of both matter and antimatter-based categories.

When applying the predictions of the Small Bang model, we're pointed towards an universe composed of 77% matter galaxies and 23% antimatter galaxies. For broader validation, this model should be applied to a more expansive dataset. Additionally, the Ulianov Theory proposes an alternate method for differentiation by examining their individual "black matter" ratios, a value close to 5.5 suggests a matter galaxy, whereas one near 3.7 indicates an antimatter galaxy. Finaly the UT gravitational model points to a antimatter g value neat to 7.7 m/s2 in the Eart surface.

While some may approach the Ulianov Theory with a dose of skepticism, its empirical foundation, coupled with the predictive insights on mass relationships, warrant attention. These revelations could reshape our understanding of galaxies and inspire renewed discourse on our universe's origins.

It's worth noting that, since 2016, the Ulianov Theory (UT) has critically assessed the efficacy of the LIGO experiment, suggesting alternative methodologies [21,22]. One such proposal endeavors to overcome the current challenges, potentially facilitating the LIGO detection of Real Gravitational Waves (RGWs), which would represent a monumental leap in gravitational wave research [23-33].

References

1. Dirac, P. A. M. (1930). A theory of electrons and protons. *Proceedings of the Royal Society of London. Series A, Containing papers of a mathematical and physical character, 126*(801), 360-365.
2. Griffiths, D. (2020). *Introduction to elementary particles.* John Wiley & Sons.
3. Thomson, M. (2013). *Modern particle physics.* Cambridge University Press.
4. Sakharov, A. D. (1998). Violation of CP-invariance, C-asymmetry, and baryon asymmetry of the Universe. In *In The Intermissions… Collected Works on Research into the Essentials of Theoretical Physics in Russian Federal Nuclear Center, Arzamas-16* (pp. 84-87).
5. Anderson, E. K., Baker, C. J., Bertsche, W., Bhatt, N. M., Bonomi, G., Capra, A., ... & Wurtele, J. S. (2023). Observation of the effect of gravity on the motion of antimatter. *Nature, 621*(7980), 716-722.
6. Ulianov, P. Y. (2012). Small Bang Creating a Universe from Nothing.
7. Ulianov, P. Y. Ulianov Sphere Network-A Digital Model for Representation of Non-Euclidean Spaces.
8. Ulianov, P. Y. (2010). Ulianov String Theory A new representation for fundamental particles. *space, 1*, 1.
9. Ulianov, P. Y. (2013). Spacetime dipole wave pressure and black holes a new way to obtain the Schwarzschild metric, without using general relativity field equations. *Asian Journal of Mathematics and Physics, 2013.*
10. Ulianov, P. Y., Freeman, A. G. (2015). Small Bang Model. A New Model to Explain the Origin of Our Universe. *Global Journal of Physics, 3*(1).
11. Freeman, A., & Ulianov, P. Y. (2012). The Small Bang Model-A New Explanation for Dark Matter Based on Antimatter Super Massive Black Holes.
12. Guth, A. H. (1981). Inflationary universe: A possible solution to the horizon and flatness problems. *Physical Review D, 23*(2), 347.
13. Tremmel, M., Governato, F., Volonteri, M., Quinn, T. R., & Pontzen, A. (2018). Dancing to CHANGA: a self-consistent prediction for close SMBH pair formation time-scales following galaxy mergers. *Monthly Notices of the Royal Astronomical Society, 475*(4), 4967-4977.
14. Lin, C. H., Chen, K. J., & Hwang, C. Y. (2023). Rapid Growth of Galactic Supermassive Black Holes through Accreting Giant Molecular Clouds during Major Mergers of Their Host Galaxies. *The Astrophysical Journal, 952*(2), 121.
15. Marconi, A., & Hunt, L. K. (2003). The relation between black hole mass, bulge mass, and near-infrared luminosity. *The Astrophysical Journal, 589*(1), L21.
16. Basu, S., & Das, A. (2019). The mass function of supermassive black holes in the direct-collapse scenario. *The Astrophysical Journal Letters, 879*(1), L3.
17. Barss, P. (2021). The mysterious origins of Universe's biggest black holes. *BBC future.*
18. Policarpo, Y. (2016). The Meaning of Time. A New Digital Complex Model of the Time. *Global Journal of Physics, 1*(2), 77-118.
19. Suh, H., Civano, F., Trakhtenbrot, B., Shankar, F., Hasinger, G., Sanders, D. B., & Allevato, V. (2020). No significant evolution of relations between Black hole mass and Galaxy total stellar mass up to z~ 2.5. *The Astrophysical Journal, 889*(1), 32.
20. Ulianov, P. Y. (2023). Excel Table, with all datasets, calculations, and graphics.
21. Ulianov, P. Y. Y., Mei, X. M., & Ping, P. Y. (2016). Was LIGO's Gravitational Wave Detection a False Alarm?. *Journal of Modern Physics, 7*, 1845-1865.
22. Mei, X., Huang, Z., Ulianov, P. Y., & Yu, P. (2016). LIGO Experiments Cannot Detect Gravitational Waves by Using Laser Michelson Interferometers—Light's Wavelength and Speed Change Simultaneously When Gravitational Waves Exist Which Make the Detections of Gravitational Waves Impossible for LIGO Experiments. *Journal of Modern Physics, 7*(13), 1749-1761.
23. Policarpo, P., & Ulianov, Y. Y. (2023). How Can we Observe Waves Without Seeing the Ocean?. *Current Research in Statistics & Mathematics, 2*(1), 55-69.
24. Regan, J. A., Downes, T. P., Volonteri, M., Beckmann, R., Lupi, A., Trebitsch, M., & Dubois, Y. (2019). Super-Eddington accretion and feedback from the first massive seed black holes. *Monthly Notices of the Royal Astronomical Society, 486*(3), 3892-3906.
25. Austin. (2023). Webb Telescope Detects Most Distant Active Supermassive Black Hole, *UT News*.
26. Volonteri, M., Madau, P., & Haardt, F. (2003). The formation of galaxy stellar cores by the hierarchical merging of

supermassive black holes. *The Astrophysical Journal, 593*(2), 661.
27. Ulianov, P. Y. (2013). An alternative to the Higgs field mass generation mechanism based on a dipole wave pressure model. *Asian Journal of Mathematics and Physics, 2013*(1), 7.
28. Ulianov, P. Y. (2016). Breaking the Paradigm of Negative Mass: Why Newton's Second Law Needs to Be Modified to Enable Newton's Gravitational Law to Deal with Antimatter. *Global Journal of Physics Vol, 4*(1).
29. Ulianov, P. Y., & Negreiros, J. P. (2015). Does the value of Planck time vary in a Black Hole Event Horizon? A new way to unify General Relativity and Quantum Mechanics. *Global Journal of Physics, 3*(1), 165-171.
30. Ulianov, P. Y. One Clue to the Proton Size Puzzle: The Emergence of the Electron Membrane Paradigm.
31. Ulianov, P. Y. (2012). Explaining the Variation of the Proton Radius in Experiments with Muonic Hydrogen.
32. Ulianov, P. Y. Rotating the Einstein's light clock, to explain the Witte Effect. A basis to make the LIGO experiment work.
33. Ulianov, P. Y. (2023). Ulianov Perfect Liquid Model Explaining why Matter Repels Antimatter.